Transient vibrational mode renormalization in dipole-coupled adsorbates at surfaces

K. Kuhnke, A. L. Harris, Y. J. Chabal, P. Jakob, and M. Morin
AT&T Bell Laboratories, 600 Mountain Avenue, Murray Hill, New Jersey 07974

(Received 6 December 1993; accepted 25 January 1994)

Dipole interactions among adsorbates at solid surfaces can strongly affect the intensities, positions, and line shapes of vibrational resonances. An understanding of these effects has been important in spectroscopic investigations of surface structure. Here, the adsorbate dipole interactions are shown to create *transient* spectral intensity and resonance position changes when vibrational modes are excited in ultrafast pump–probe laser experiments at surfaces. The spectral changes occur because the intensities and positions of vibrational resonances are dependent upon the magnitude of interadsorbate dipole interactions, and vibrational excitation modifies the effective oscillator dynamic dipoles that determine these interactions. The vibrational modes are different (renormalized) after excitation because of the change in coupling. The effects account for unusual spectral transients observed in recent pump–probe experiments on the Si–H stretching modes of vicinal H/Si(111) surfaces [K. Kuhnke, M. Morin, P. Jakob, N. J. Levinos, Y. J. Chabal, and A. L. Harris, J. Chem. Phys. **99**, 6114 (1993)]. The predicted effects serve as a novel time-resolved probe of the strength of dipolar interactions in adsorbate layers, and will arise in any adsorbate layer where the vibrational dynamic dipole interactions are large enough to cause spectral intensity borrowing among different adsorption sites or different adsorbates.

I. INTRODUCTION

Dipole interactions among adsorbates at solid surfaces are often important in determining the intensities, positions, and line shapes of vibrational resonances.[1–6] An understanding of these effects has been important in using vibrational spectroscopy as a quantitative tool for investigations of surface structure.[7] Ultrafast dynamic studies of adsorbate vibrational responses, such as recent studies of vibrational energy flow in adsorbate/surface systems,[8–14] introduce a new aspect of this problem. In such studies, changes in the vibrational spectrum of the system are measured following vibrational excitation of a selected vibrational mode. In particular, in recent studies of stepped vicinal H/Si(111) surfaces with multiple Si–H stretching normal modes, the spectral changes have been interpreted in terms of energy diffusion among the vibrational modes.[13,14] However, vibrational excitation of a mode modifies the vibrational polarizability of the oscillators involved in the mode, and instantaneously changes the dipole interactions in the adsorbate layer. The characteristic normal modes of the surface are therefore changed, or renormalized, by vibrational excitation. In this article we show that the excitation-induced renormalization of the vibrational modes produces transient spectral resonance intensity changes and resonance line shifts in pump–probe experiments of systems with several spectroscopically active normal modes. The spectral changes can mimic the spectral saturation that occurs upon vibrational excitation and therefore can affect the interpretation of dynamic experiments. In addition, the magnitude of the transient spectral changes can, when interpreted correctly, give a measure of the strength of the dipole coupling among oscillators.

We present a model to calculate the spectral effects of renormalization and apply it in particular to the transient spectroscopy of Si–H stretching modes of a stepped vicinal H/Si(111) surface, which has monohydride-terminated terraces and dihydride-terminated steps.[14] The calculation is shown to qualitatively account for unusual spectral effects observed in recent pump–probe measurements of vibrational energy flow on that surface,[14] and the predicted effects are large enough to modify conclusions about the Si–H vibrational energy flow kinetics. The model that we present assumes that vibrational dephasing occurs prior to the spectral probing process, and that the coherent vibrational exciton site-to-site hopping rate is small compared to the dephasing rate so that vibrational excitations can be treated as quasilocalized and incoherent. These assumptions appear to be appropriate for Si–H oscillators. Our approach is similar to that of Persson,[15] who recently applied these assumptions to calculate the excited state spectrum of the flat H/Si(111) surface.

The assumption of complete loss of phase coherence among oscillators is itself a source of energy transfer among modes since several modes involve different motions of the same set of oscillators. This is, however, a minor effect in the present case, since the degree of overlap is small. The spectral changes discussed here, both from renormalization as well as from the less important mixing of energy among modes by dephasing, are complete on the time scale of vibrational dephasing [$\sim$10 ps for H/Si(111) at 300 K]. They are rapid compared to interoscillator energy diffusion by incoherent dipole–dipole spatial energy transfer, which is believed to occur on this surface on time scales of $>$100 ps.[13,14] The slower incoherent energy diffusion itself has been previously modeled,[13] and is not treated here.

Effects discussed here may also occur following vibrational excitation of a single isotopic component in an isotopically mixed adsorbate system, or in excitation of one subset of adsorption sites on a surface with multiple adsorption sites. The assumption of quasilocalized, incoherent excita-

 0021-9606/94/100(9)/6896/11/$6.00

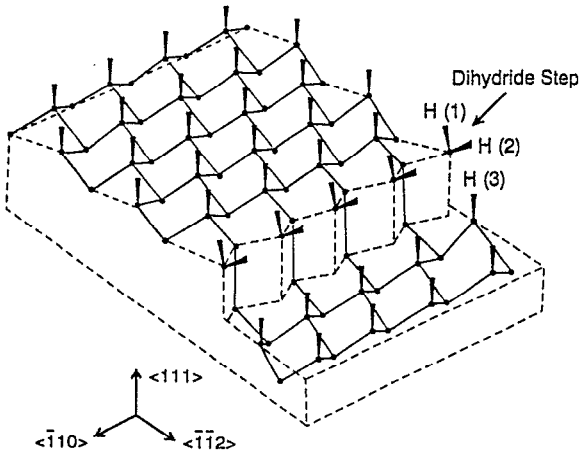

FIG. 1. Surface and adsorbate geometry of the chemically prepared hydrogen-terminated vicinal Si(111) surface miscut in the $\langle\bar{1}\bar{1}2\rangle$ direction. Steps are terminated by dihydrides. H(1), H(2), and H(3) label the Si–H bonds involved in the three step modes. The 9° miscut discussed in this paper gives terraces with an average of 4.3 rows of Si–H oscillators, neglecting H(3) which becomes part of the step modes. Reproduced from Ref. 13.

tions used here may, however, not be appropriate for calculations where the interadsorbate coupling is very strong, or where the dynamics are probed on a time scale short compared to the dephasing time (e.g., CO/metal),[9,11] and different methods for the calculation of the spectral transients may then be needed.

The dynamic experiments on stepped H/Si(111) surfaces are briefly described in Sec. II. The method for calculation of transient renormalization is described in Sec. III, starting with a homogeneous surface, and then extending to the case of multiple oscillator types consisting of rows of different oscillators, intended to model the stepped vicinal H/Si(111) surface. Section IV describes the calculation of the Si–H stretching normal modes of the stepped surface, and their changes upon vibrational excitation, and compares the results with recent experiments.

II. INFRARED PUMP–PROBE EXPERIMENTS ON STEPPED H/Si(111)

Several results of picosecond experiments used to measure vibrational energy diffusion among the Si–H stretching modes on hydrogen-terminated, stepped vicinal Si(111) surfaces are summarized.[13,14] Throughout we focus on surfaces cut 9° from the (111) plane along the $\langle\bar{1}\bar{1}2\rangle$ azimuth. The geometry of such a surface[13,14,16] is shown in Fig. 1. It has monohydride-terminated (111) terraces with an average width of 5.3 rows of surface silicon atoms, and dihydride-terminated steps. An infrared absorption spectrum[16] of this surface in the region of the Si–H stretching modes shows four resonances (Fig. 2). The mode labeled A is localized on the terrace, and the three modes labeled C_1, C_2, and C_3 are localized near the steps, involving primarily motions of H(1), H(3), and H(2), respectively, in Fig. 1. A more detailed discussion of the mode assignments is deferred to Sec. IV.

Dynamic experiments to determine the extent and rate of vibrational energy flow among the Si–H oscillators of the surface are carried out by pumping a vibrational normal mode with a short, intense infrared pulse, and probing the same or other vibrational modes by vibrational spectroscopy as a function of delay after the pump.[13,14] In the present case, the modes are probed by sum frequency generation (SFG) spectroscopy, whose vibrationally resonant signal on any

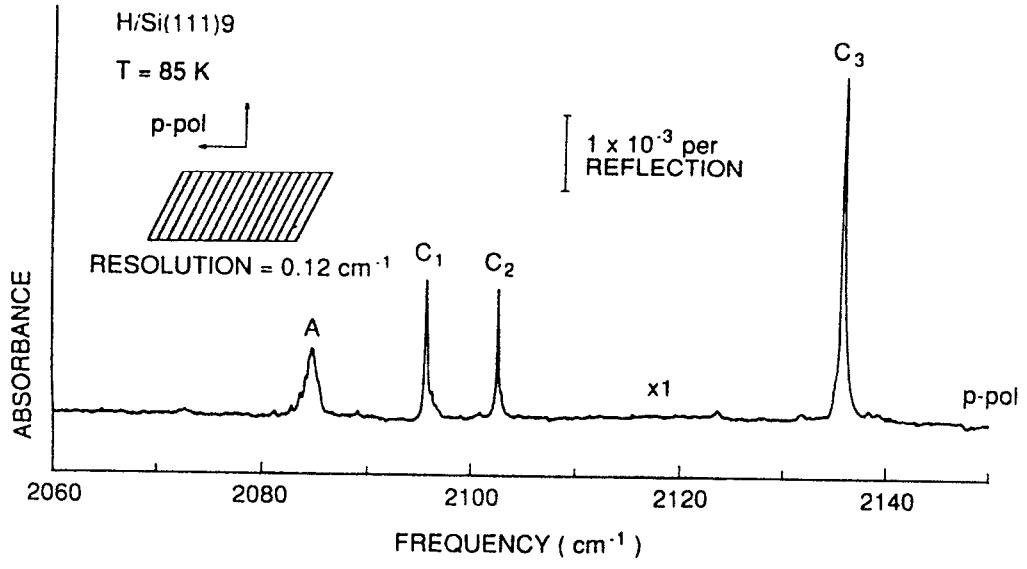

FIG. 2. Infrared absorption spectrum of H/Si(111) 9°, taken at 90 K by attenuated total internal reflection spectroscopy with *p*-polarized infrared light, and with the scattering plane perpendicular to the step edge. Reproduced from Ref. 16.

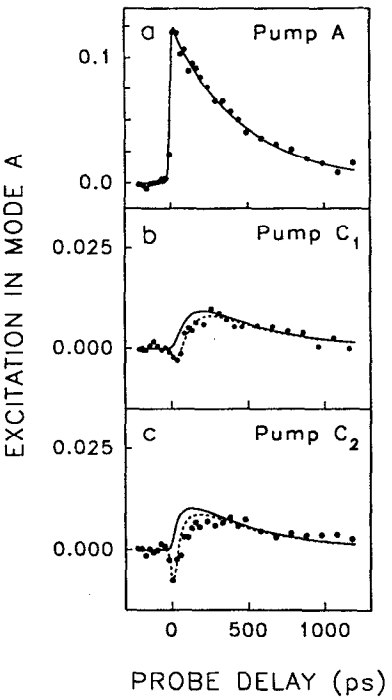

FIG. 3. Transient apparent excitation n_1(obs) on the dihydride-stepped vicinal H/Si(111) 9° surface with the SFG probe set to the A mode. The IR pump is set as labeled on each graph. Solid points: experimental data; solid lines: results of a kinetic model described in Ref. 14. Dashed lines: include a transient negative excitation component proportional to the instantaneous excitation in the step modes, whose lifetimes are much shorter than that of the A mode. Reproduced from Ref. 14.

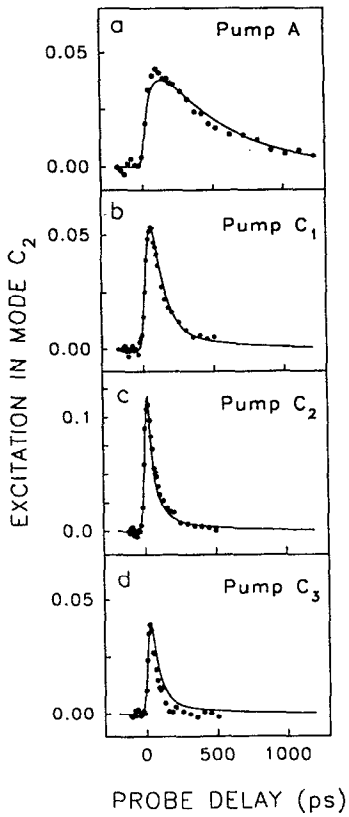

FIG. 4. Excitation transients of the dihydride-stepped surface with the SFG probe set to the C_2 mode. Solid points: experimental data; solid lines: results of a kinetic model described in Ref. 14. Reproduced from Ref. 14.

particular mode is proportional to $(n_0-n_1)^2$, where n_0 and n_1 are the fractional populations of the ground and excited states of the probed transition. Thus the SFG signal decreases when population is moved from the ground to the excited level, and the apparent observed fractional excitation n_1(obs) of a probed mode can be extracted by[14]

$$n_1(\text{obs})=\frac{1-r^{1/2}}{2},$$

where

$$r=\frac{S(\tau_d)}{S_0}, \tag{1}$$

and where $S(\tau_d)$ is the SFG signal at delay τ_d from the pump, and S_0 is the signal with no pump present, and we have assumed that $n_0+n_1=1$. Data calculated in this way for the transient excitation which appears in the A and C_2 modes following an infrared pump pulse resonant on various normal modes of the dihydride-stepped surface are shown in Figs. 3 and 4.

The excitation levels in Figs. 3 and 4 for the A and C_2 modes, shown as a function of probe delay from the pump, generally show positive excitation levels, no matter which mode is pumped. This illustrates that energy flow from one mode to another can be mapped using the pump–probe technique. The decay of excitation, with decay times ranging from 60 to 500 ps, results from different energy flow rates out of the probed mode into both substrate phonons and into other vibrational modes of the overlayer. General conclusions about the energy flow on the stepped H/Si(111) surfaces can be formed simply based upon the decay kinetics of the various modes. In more detail, however, it is appealing to assume that the observed transients are all direct measures of the energy transferred into the various modes. Under this assumption, the data were used[14] to construct a kinetic model, which gives the solid line fits to the data in Figs. 3 and 4.

However, vibrational renormalization can also lead to intensity changes of all normal modes after excitation of one, even in the absence of substantial energy transfer. As an example, note that in Fig. 3, when mode C_1 or C_2 is pumped and mode A is monitored, there is a negative spike in the excitation plot at early time. This corresponds to an SFG signal increase on mode A, which cannot be accounted for by energy transfer into mode A. The transient lasts as long as the step modes remain excited, and the dashed lines in Fig. 3(b) and 3(c) add an arbitrary negative spike on the excitation plot proportional to the time-dependent energy in the step modes. The renormalization model in the following sections will account for these negative transients, and also predicts that positive excitation transients can arise from renormalization. The positive transients are predicted to contribute substantially in at least some cases to the transients shown in

Figs. 3 and 4 and therefore to obscure the detailed energy flow kinetics.

III. RENORMALIZATION AFTER VIBRATIONAL EXCITATION

The calculations will refer to the integrated infrared absorption intensity A of the normal modes of the adsorbate layer. This absorption is proportional to the square of the normal mode effective dipole, which is in turn obtained from the vector sum of the amplitudes of all oscillators in the normal mode, under the assumption that the external field and the bond dipole derivatives are the same at all sites. Upon vibrational excitation, the apparent excitation of a normal mode is calculated from the saturation of the absorption by

$$n_1(\text{obs})=\frac{1}{2}\left(1-\frac{A'}{A}\right), \tag{2}$$

where A and A' are the integrated absorbance of the ground state and excited systems, respectively. The apparent excitation is a useful quantity to characterize signal changes, even if they derive from renormalization effects, and will be used throughout. The experiments discussed in Sec. II, however, involve an SFG probe. The SFG signal scales as the product of the infrared and Raman polarizations of a mode. The excitation calculated from SFG [Eq. (1)] thus scales as the square root of this product. Under the assumption that the visible probe field used in SFG and the Raman bond polarizabilities are uniform at all surface sites, and that the Raman bond polarizability for each Si–H bond is highly anisotropic along the bond, then the infrared and Raman polarizations in a normal mode scale together as the vector sums of the motions of the Si–H bonds in that mode. In that case the excitation observed in SFG [Eq. (1)] and the excitation observed in infrared absorption [Eq. (2)] are the same. Both the assumption of uniform visible probe field and the assumption of highly anisotropic bond polarizability are roughly true, based upon the results of recent surface Raman spectroscopy on the H/Si(111) surface.[17,18] We will assume henceforth that the apparent excitation calculated from the normal modes is the same for infrared and SFG probes.

The model is focused on application to the stepped H/Si(111) surface, and several approximations are introduced which are appropriate for that system. Vibrational excitation is assumed to largely remain within one subset of oscillators, for instance on the terrace, for a time long compared to the dephasing time of the vibrational modes (which is ~10 ps at room temperature for the Si–H modes). Then, if the coherent vibrational exciton hopping rate between sites is slow compared to the dephasing time, which appears to be valid for Si–H modes at room temperature,[15] the vibrational excitation can be considered to be localized randomly on individual oscillators.

The changes in the normal modes induced by vibrational excitation are calculated for a system consisting of several types of oscillators. In the present case, each row of Si–H oscillators parallel to a step edge will be considered a different oscillator type. In general, the types might be isotopically different molecules or different adsorption sites. The calculation takes two parts. First, the effective vibrational polarizability of each type of oscillator is determined based upon its degree of vibrational excitation. Second, the normal modes of the surface are determined by diagonalizing the potential energy matrix using the effective vibrational polarizabilities in the dipole interaction terms. In Sec. III A the effective vibrational polarizability of a vibrationally excited oscillator type is discussed. In Sec. III B, the infrared active normal modes of a ground state system of interacting rows of oscillators is developed using a potential energy matrix which condenses the $k=0$ mode of each row into a single element (row-as-oscillator) to simplify calculation. Section III C combines these to calculate the changes in the normal modes upon vibrational excitation.

A. Effective polarizability of a vibrationally excited system

For a uniform adlayer in the vibrational ground state, the spectroscopic response is determined by starting with the molecular, or site, complex polarizability of a ground state oscillator[6,19]

$$\alpha_0(\omega)=\alpha_e+\frac{b}{(\omega_0^2-\omega^2)-i\gamma\omega}. \tag{3}$$

Here α_e is the electronic polarizability, ω_0 and γ are the frequency and damping of the ground state transition, and $b=(e^*)^2/m^*=\omega_0^2\alpha_v$, where e^* and m^* are the effective charge and mass of the oscillators, and α_v is the zero frequency vibrational polarizability of the ground state. The spectroscopic response of the uniform layer to an external driving field E_0 must include the interaction among the dipoles in the layer. For a homogeneous layer, the induced dipole moment is the same at every site in the infrared active $k=0$ vibrational mode,

$$p(\omega)=\alpha(\omega)\left[E_0-\sum_{i\neq j}U_{ij}p(\omega)\right]\equiv\alpha_{\text{eff}}(\omega)E_0, \tag{4}$$

where U_{ij} is the geometric factor in the dipole interaction,

$$U_{ij}=\frac{1+\kappa}{r_{ij}^3},$$

$\kappa=\epsilon-1/\epsilon+1$ is the magnitude of the image dipole (dipoles normal to the surface), and ϵ is the dielectric constant of the substrate ($\epsilon=11.7$ for silicon).

Equation (4) defines the effective layer polarizability α_{eff}. The absorption of the overlayer is determined by $\text{Im}[\alpha_{\text{eff}}(\omega)]$. Solving for $\alpha_{\text{eff}}(\omega)$ in Eq. (4), and substituting from Eq. (3),

$$\text{Im}[\alpha_{\text{eff}}(\omega)]=\frac{\gamma\omega\omega_0^2}{\{\omega_0^2[1+U(0)\alpha_v/\epsilon_\infty]-\omega^2\}^2+\gamma^2\omega^2}\left(\frac{\alpha_v}{\epsilon_\infty^2}\right), \tag{5}$$

where $U(0)$ is the lattice sum of U_{ij} for $k=0$ [equal to $11.0(1+\kappa)/a^3$ for a hexagonal lattice with lattice constant a, assuming perpendicular dipoles], and the quantity $\epsilon_\infty=1+U(0)\alpha_e$ represents the effective dielectric screening of fields by the layer. Equation (5) illustrates the two primary

effects of the dipole interactions among oscillators in a homogeneous layer.[19] First, there is a resonance frequency shift of $\Delta\omega \sim U(0)\alpha_v/2\epsilon_\infty$ of the $k=0$ mode from the frequency of the isolated oscillators, due to interaction of the vibrational dynamic dipole moments. Second, the vibrational polarizability is screened by an effective dielectric response arising from the electronic polarizability of the adsorbates, which reduces the absorption for perpendicular dipoles by $(1/\epsilon_\infty)^2$.

How is the spectrum of the homogeneous overlayer altered upon vibrational excitation? For quasilocalized, incoherent excitations, the vibrationally excited system can be considered as a random mixture of two types of oscillators, with vibrational polarizabilities α_0 and α_1, where α_0 is again the vibrational polarizability of the ground state oscillator [Eq. (3)] and α_1 is the vibrational polarizability of the excited state oscillator.[15]

$$\alpha_1(\omega)=\alpha_e+\frac{2b}{[(\omega_0-\Xi)^2-\omega^2]-i\gamma\omega}-\frac{b}{(\omega_0^2-\omega^2)-i\gamma\omega}. \tag{6}$$

Here, Ξ is the anharmonic shift of the excited state transition. The first vibrational term in α_1 gives rise to the excited state absorption which is shifted by the bond anharmonicity from the frequency of the ground state transition, and the second vibrational term is the source of emission from the excited state, at the same frequency as the ground state absorption. It is assumed that the electronic polarizability is unaltered by vibrational excitation.

For a system of randomly localized excitations, the effective polarizability of the layer after excitation can be calculated by methods used for a random mixture of two isotopes. The usual method is to introduce an effective single site polarizability. The simplest approximation for that polarizability is the average polarizability approximation[6]

$$\alpha(\omega)=c\alpha_1(\omega)+(1-c)\alpha_0(\omega)=\alpha_e+c\frac{2b}{(\omega_0-\Xi)^2-\omega^2-i\gamma\omega}+(1-2c)\frac{b}{\omega_0^2-\omega^2-i\gamma\omega}, \tag{7}$$

where c is the fraction of excited state molecules in the layer.

When the anharmonic shift Ξ is large, the magnitude of either vibrational term in Eq. (7) is small in the resonance region of the other, and this results in two essentially independent resonances in the overlayer when $\mathrm{Im}[\alpha_{\mathrm{eff}}(\omega)]$ is determined, arising from the ground state and excited state transitions. This is the appropriate limit for Si–H bonds, where $\Xi \sim 60\ \mathrm{cm}^{-1}$, compared to a linewidth and dipole interaction of a few cm^{-1} or less. The ground state resonance is then obtained simply by substituting $(1-2c)\alpha_v$ for α_v in Eq. (5). First, this leads to the obvious reduction of the ground state absorption signal by a factor $(1-2c)$ [consistent with the integrated absorption scaling as n_0-n_1 or $(1-c)-c=1-2c$]. Second, the resonance line shift of the $k=0$ mode is reduced from $\Delta\omega \sim U(0)\alpha_v/2\epsilon_\infty$ in the ground state system to $\Delta\omega \sim (1-2c)U(0)\alpha_v/2\epsilon_\infty$ in the vibrationally excited system. Similar effects occur for the excited state transition: the strength grows as c, and the resonance position of the transition shifts as more oscillators are excited.

The essential point is that, within the average polarizability approximation, and for a large anharmonic shift of the excited state transition, the effect of vibrational excitation of a fraction c of the oscillators can be described by a reduction in α_v of each oscillator to a value $(1-2c)\alpha_v$. Thus, in the region of the ground state transition, which is the concern here, excitation can be approximated by the substitution $\alpha_v \Rightarrow (1-2c)\alpha_v$. Note that since $\alpha_v=(e^*)^2/\omega_0^2 m^*$, this reduction is equivalent to a change of e^* by the square root of $(1-2c)$: $e^* \Rightarrow (1-2c)^{1/2}e^*$.

The emphasis in the calculations that follow is on changes in integrated line intensities and line shifts. The simple average polarizability approximation used here has previously been shown to give accurate values for these properties in isotopically mixed overlayers, and will be used in the calculations. It does not, however, reproduce line shapes well, because it does not include inhomogeneities which arise from random distributions of the different oscillators. Persson has applied a more accurate coherent potential approximation to calculate the spectrum of the vibrationally excited flat H/Si(111) surface.[15] Such methods could be applied, at the cost of complexity, to calculate spectral changes on the multiple normal modes of the stepped vicinal H/Si(111) surface considered here, when detailed experimental data justifies the effort.

B. Interactions among oscillator rows

To calculate the infrared active normal modes of the stepped surface, each row of Si–H oscillators parallel to the step edge in Fig. 1 is treated as one oscillator type.[20] Each oscillator row i, for instance H(1), H(2), or H(3) in Fig. 1, has a characteristic frequency for its in-phase infrared active mode, $\omega_{\mathrm{row}\ i}$. The interactions between the rows to form normal modes of the surface are calculated by diagonalizing the potential energy matrix of the system. The normal mode calculation will be set up for the case of two interacting rows, to simplify presentation. The extension to the multiple rows of the unit cell of the stepped surface is straightforward, and is discussed in Sec. IV. In this section, the results for the ground state are illustrated. In Sec. III C, the modifications due to vibrational excitation are outlined.

Consider the interaction between the $k=0$ modes of two adjacent oscillator rows, with oscillator vibrational coordinates z_1 and z_2, effective charges e_1^* and e_2^* zero-order frequencies ω_{01} and ω_{02}, and identical reduced masses m, embedded in a dielectric layer with dielectric constant ϵ_∞. Figure 5 illustrates, for instance, the geometry of two rows of Si–H oscillators parallel to the step edges of the dihydride-stepped vicinal H/Si(111) surface. The frequencies of the in-phase vibrations of the rows are shifted from the frequency of the isolated oscillators by $\Delta\omega_i=\omega_{\mathrm{row}\ i}-\omega_{0i} \sim \omega_{0i}U_{\mathrm{row}}(0)\alpha_{vi}/2\epsilon_\infty$ where α_{vi} is the zero frequency vibrational polarizability of the oscillators in row i, and the dipole sum $U_{\mathrm{row}}(0)$ is analogous to $U(0)$ in Sec. III A, but the sum

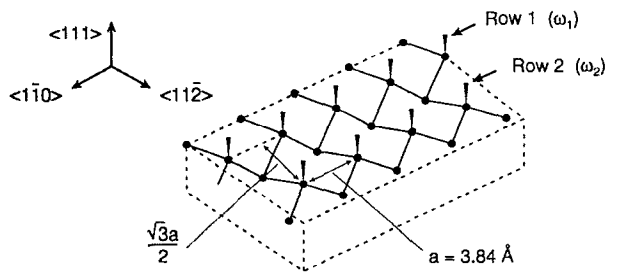

FIG. 5. Geometry of Si–H oscillator rows on (111) terraces of the vicinal H/Si(111) surface shown in Fig. 1, used to model dipole interactions between rows with different frequencies in Secs. III B and IV A of the text. The oscillator rows are parallel to the $\langle\bar{1}10\rangle$ crystal axis.

is only over one row. For a row of perpendicular dipoles with uniform separation between oscillators of lattice constant a, $U_{\text{row}}(0)=2.40(1+\kappa)/a^3$. The interaction of the dynamic dipole moments between the $k=0$ modes of the two rows adds a potential energy term per oscillator of $f_{12}z_1z_2$, where f_{12} is the coupling factor

$$f_{12}=\frac{U_{1\text{row}2}(0)e_1^*e_2^*}{\epsilon_\infty} \quad \text{and} \quad f_{21}=f_{12}, \tag{8}$$

where $U_{1\ \text{row}\ 2}(0)$ is a sum of U_{ij} between one oscillator in row 1 and all the oscillators of row 2 for the $k=0$ modes of each row. For the rows shown in Fig. 5, for instance, $U_{1\ \text{row}\ 2}=2.59(1+\kappa)/a^3$, where a is again the lattice constant of the hexagonal H/Si(111) lattice. The normal modes of the interacting rows (for $k=0$ along the rows) are obtained by treating the $k=0$ mode of each row as a single oscillator (row-as-oscillator). The potential energy for the in-phase modes of the coupled rows can then be written $(m/2)\mathbf{z}^T\mathbf{:M:z}$ where $\mathbf{M}$ is the matrix

$$\mathbf{M}=\begin{pmatrix} \omega_{\text{row1}}^2 & \frac{f_{12}}{m} \\ \frac{f_{21}}{m} & \omega_{\text{row2}}^2 \end{pmatrix} \tag{9}$$

and $\mathbf{z}$ is the column vector $\binom{z_1}{z_2}$.

The normal coordinates which diagonlize $\mathbf{M}$ are obtained by finding the matrix $\mathbf{U}$ such that $\mathbf{U}^{-1}\mathbf{MU}=\mathbf{D}$ where $\mathbf{D}$ is a diagonal matrix. Then the elements D_{ii} are the eigenvalues of $\mathbf{M}$, $\omega_{(+-)}^2$ and the columns of $\mathbf{U}$ are the eigenvectors of $\mathbf{M}$, the normal coordinates of the system $q_{(+-)}$. The eigenvalues are

$$\omega_{\pm}^2=\frac{1}{2}\ (\omega_{\text{row1}}^2+\omega_{\text{row2}}^2)\pm\frac{1}{2}\left[(\omega_{\text{row1}}^2-\omega_{\text{row2}}^2)+4\left(\frac{f_{12}}{m}\right)^2\right]^{1/2}. \tag{10}$$

In the symmetric case that the two rows have identical initial frequencies, $\omega_{\text{row}\ 1}=\omega_{\text{row}\ 2}=\omega_0$, the frequency shifts are $(+/-)f_{12}/2m\omega_0^2$, and the eigenvectors are in-phase and out-of-phase vibrations of the two rows, with all the absorption strength in the higher frequency in-phase mode. For the asymmetric case $\omega_2>\omega_1$, we define a coupling parameter β,

$$\beta=\frac{f_{12}}{m(\omega_{\text{row2}}^2-\omega_{\text{row1}}^2)}. \tag{11}$$

Assuming weak dipole coupling, $\beta\ll 1$, then the frequency ω_+ and normal coordinate q_+ are small perturbations of $\omega_{\text{row}\ 2}$ and z_2, respectively, and the frequency ω_- and normal coordinate q_- are small perturbations of $\omega_{\text{row}\ 1}$ and z_1. Defining the frequency shifts $\Delta\omega_+=\omega_+-\omega_{\text{row}\ 2}$ and $\Delta\omega_-=\omega_--\omega_{\text{row}\ 1}$,

$$\frac{\Delta\omega_+}{\omega_{\text{row2}}}=\beta\frac{f_{12}}{2m\omega_{\text{row2}}^2}, \quad \frac{\Delta\omega_-}{\omega_{\text{row1}}}=-\beta\frac{f_{12}}{2m\omega_{\text{row1}}^2},$$
$$q_+=\frac{\beta}{\sqrt{1+\beta^2}}\ z_1+\frac{1}{\sqrt{1+\beta^2}}\ z_2, \tag{12}$$
$$q_-=\frac{1}{\sqrt{1+\beta^2}}\ z_1-\frac{\beta}{\sqrt{1+\beta^2}}\ z_2.$$

The relative absorbances A_+ and A_- of the two modes are obtained directly from the normal coordinates in Eq. (12), and are $A_+=A_0(1+\beta)^2/(1+\beta^2)$ and $A_-=A_0(1-\beta)^2/(1+\beta^2)$, where A_0 is the absorbance of either row without coupling (assuming $e_1^*=e_2^*$). Since the two oscillators are in-phase for q_+ and out-of-phase for q_-, the higher frequency normal mode gains absorbance at the expense of the lower frequency mode, with conserved total absorbance. This is the well-known intensity borrowing effect.[7] The fraction of the vibrational energy on the majority and minority oscillators in a given mode are $1/(1+\beta^2)$ and $\beta^2/(1+\beta^2)$, respectively. Note that since β is assumed small, meaning that the intrinsic frequency separation of the rows is large compared to the dipole interaction, the frequency shifts caused by interaction between the two rows are small compared to the self-shift of each row's $k=0$ mode from the frequency of its isolated oscillators.

C. Vibrational excitation of interacting oscillator rows

Combining the approaches of the last two sections, the changes in the normal modes of the interacting rows after vibrational excitation of any one normal mode can now be calculated. Upon excitation, each row is treated as a uniform set of oscillators as in Sec. III A; the e^* of each row is modified based upon the extent of vibrational excitation of that row. The interactions among the in-phase modes of the rows are then recalculated as in Sec. III B, and the new normal modes of the surface are obtained. The changes in the integrated intensities and frequency positions directly follow. To estimate the degree of vibrational excitation in each row, we assume complete vibrational dephasing, both within each row and between rows, after the vibrational pumping process. The excitation is then localized on each row with a probability given by the fraction of the vibrational energy which is on that row in the pumped normal mode.

Explicitly, the normal modes of the system are first calculated as in Sec. III B using the ground state value of e^* for each row. A normal mode x to be excited is chosen and the

fraction P_{ix} of its vibrational energy which is on each row i is calculated. This fraction is obtained explicitly from the square of the amplitude of the vibrational motion of the row i in the normal mode x which is to be pumped. Then for a fractional excitation of mode x given by n_{1x}, the fractional excitation of each oscillator row i is $c_{ix}=P_{ix}n_{1x}$. The effective charge of the oscillators in row i is then modified by the factor $(1-2c_{ix})^{1/2}$, the normal modes are recalculated, and the absorbance change of each mode is obtained. The changes in the absorbances will be discussed in terms of the apparent excitation n_1(obs) [Eq. (2)]. Changes in the positions of the vibrational resonances can also be calculated.

This is illustrated with the two row model of the last section. Consider excitation of mode q_+, with an excitation, n_{1+}. The concentrations of excited oscillators on rows i, $c_{i+}=P_{i+}n_{1+}$ are $c_{1+}=n_{1+}[\beta^2/(1+\beta^2)]$ and $c_{2+}=n_{1+}[1/(\beta^2+1)]$, from Eq. (12). Designating properties of the excited system by a prime ($'$) the effective charges of the rows in the excited system are $(e_i^*)' = (1-2c_{i+})^{1/2}e_i^*$. The primary effect of this change is to modify the interrow coupling in the excited system: $f'_{12}=U_{1\ \mathrm{row}\ 2}(e_1^*)'(e_2^*)'/\epsilon_\infty$. It also modifies the zero-order row frequencies, $\Delta\omega_i' = \omega'_{\mathrm{row}\ i} - \omega_{0i} = U_{\mathrm{row}}(0)\alpha'_{vi}/2\epsilon_\infty$ where $\alpha_i' = (1-2c_{i+})\alpha_{vi}$. Both changes affect the interaction parameter in the excited system

$$\beta'=\frac{f'_{12}}{m[(\omega'_{\mathrm{row2}})^2-(\omega'_{\mathrm{row1}})^2]}. \tag{13}$$

The new normal coordinates after excitation, q'_+ and q'_-, are calculated from Eq. (12) using β' in place of β. The changes in the intensities of the normal mode resonances are determined by both the changes in the vibrational amplitudes of the rows determined by β' and by the changes in the effective charges of the rows in the excited state $(e^*)'$. In the present example, for instance, the integrated absorbance of the q_- mode after vibrational excitation of the q_+ mode, is

$$A'=\frac{[\sqrt{1-2c_{1+}}-\beta'\sqrt{1-2c_{2+}}]^2}{1+(\beta')^2}\ A_0 \tag{14}$$

contrasted with the ground state value $A=A_0(1-\beta)^2/(1+\beta^2)$. To first order in β, the excitation of the q_+ mode leads to a renormalization transient on the q_- mode of $n_{1-}(\mathrm{obs})\sim-2\beta n_{1+}$. In the reverse case, the apparent excitation of the q_+ mode after pumping the q_- mode is $n_{1+}(\mathrm{obs})\sim+2\beta n_{1-}$ for small β. Both of these occur in the absence of substantial intermode energy transfer, and are renormalization effects.

We note, however, that a consistent interpretation of the above result does indicate that some instantaneous energy transfer has occurred between modes. This is because in order to carry out the calculation assuming complete dephasing, we have projected the energy of the pumped normal mode incoherently onto each oscillator row. If this energy distribution is projected back onto the starting normal modes, without renormalization, some energy appears in the mode that was not directly pumped and a slight reduction of the energy in the pumped mode is observed. This effect is small as long as β is small. In order to be consistent, when discussing an excitation of, for instance, 10% the level of excitation of a normal mode x will be chosen so that after dephasing the projection of the energy back onto the pumped mode (before renormalization) gives a chosen excitation level $n_{1x}^0=0.1$. In the case of two interacting rows, this leads to a projection of energy into the other mode of $n_{1y}^0\sim2\beta^2n_{1x}^0$ whose magnitude is less than the renormalization effect (which is approximately linear in β) for small β. In the results of Sec. IV, the calculated renormalization effect is compared to this incoherent projection of energy among modes. The renormalization dominates the intensity changes of the modes that are not directly excited.

IV. H/Si(111)

In Sec. IV A, these relations are applied to an example of two interacting rows of Si–H oscillators with characteristic parameters, in order to illustrate the order of magnitude of the expected effects for the H/Si(111) system. In Sec. IV B, the model is applied to calculate both the ground state normal modes, and the changes in the normal modes upon vibrational excitation, for stepped H/Si(111) surfaces.

A. Interacting rows on a Si(111) terrace

We consider two rows of Si–H oscillators on a H/Si(111) terrace, parallel to the dihydride-terminated step edge in Fig. 1 (rows oriented along the $\langle\bar{1}10\rangle$ direction). The assumed geometry is illustrated in Fig. 5. The effective charges of the oscillators are as in the real system, but the frequency separation between the intrinsic frequencies of the two rows is arbitrarily set to 10 cm^{-1} to roughly model the characteristic frequency separations of step and terrace modes on the stepped vicinal H/Si(111) surface. The oscillators of the terrace are oriented perpendicular to the terrace, arranged in a hexagonal lattice with lattice constant $a=3.84$ Å. The separation between oscillators along the row is a, and the separation between rows is $a\sqrt{3}/2$. The unscreened effective charge of Si–H oscillators on the flat surface[21] is $e^*/e=0.24$. It is assumed that all dipoles are placed into a thin dielectric layer with an effective dielectric constant of ϵ_∞. The experimental value[20] of ϵ_∞ is approximately 2. The interaction parameter between the rows is

$$f_{12}=\frac{U_{1\mathrm{row2}}(0)(e^*)^2}{\epsilon_\infty}=560\ \ \mathrm{dyn/cm}. \tag{15}$$

This choice of parameters gives a shift of the in-phase mode for the flat H/Si(111) surface, $\Delta\omega\sim U(0)\alpha_v/2\epsilon_\infty$, of 9.6 cm^{-1}. This is consistent with the value of 9 cm^{-1} measured by electron-energy-loss spectroscopy (EELS).[22] Note however that it is 1.8 times larger than the coupling used in Refs. 20 and 21 where image effects were not explicitly included. The row frequency for row 1 is set to $\nu_{\mathrm{row1}}=\omega_{\mathrm{row1}}/(2\pi c)=2075\ \mathrm{cm}^{-1}$, and the row frequency of row 2 is set 10 cm^{-1} above this. The coupling parameter β is then $\beta=0.227$. When the intensities of the normal modes are calculated, intensity borrowing is found to be a strong effect, with $A_+/A_-=[(1+\beta)/(1-\beta)]^2\sim2.5$. In contrast, the fraction of the vibrational energy of the normal modes which is on the minority oscillator $\beta^2/(1+\beta^2)$ is still only ~5%, so that

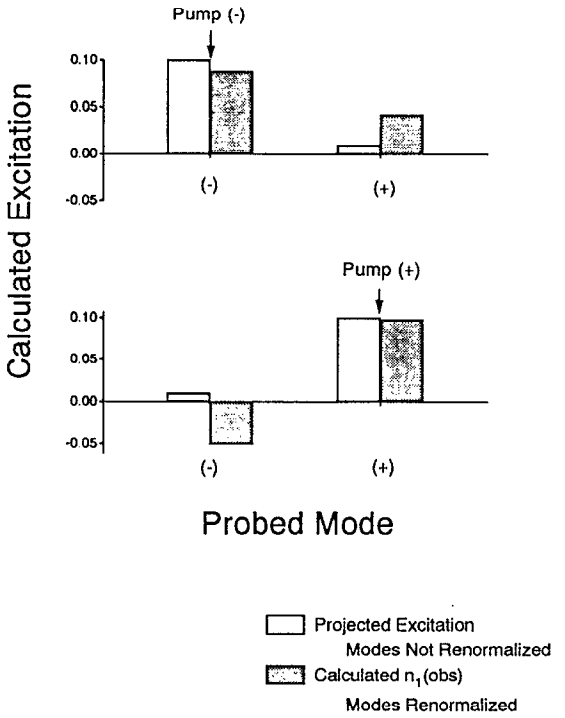

FIG. 6. Calculated excitation of the Si–H normal modes of the two row system of Fig. 5 after (a) pumping the (−) mode and (b) pumping the (+) mode. Each mode is assumed pumped to a zero-order excitation of 0.10. The frequency gap between the two rows is set to 10 cm^{-1}, and the interaction parameter β is 0.23. Unshaded columns: excitation projected into each zero-order mode by the assumption that all oscillators lose phase coherence after the pumping process; shaded columns: the apparent excitation n_1(obs) which would be observed in a transient experiment by an absorption probe following mode renormalization.

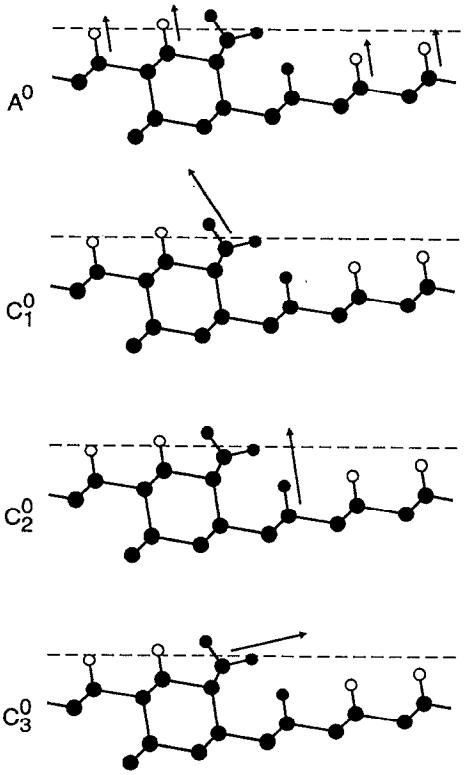

FIG. 7. Zero-order normal modes of the dihydride-stepped vicinal H/Si(111) 9° surface, before terrace-step dipole coupling is included. Step modes C_i are assumed to be vibrations of single bonds (see the text).

the mode energy is still well-localized on the majority oscillator. The self-shift of the row frequencies from the isolated oscillator frequencies is +2.1 cm^{-1} for each row. The shift due to coupling between the two rows is much smaller, less than 0.1 cm^{-1}, because of the frequency gap between the rows.

The effect of vibrational excitation on the vibrational spectrum of the two row system in the asymmetric case is calculated according to the method in Sec. III C. A level of excitation of one normal mode x, n_{1x}, is chosen so that after complete dephasing the projection of the energy back onto the same mode n^0_{1x} is 0.10. The results for the apparent excitation of each mode after renormalization, n_1(obs), as well as the incoherent projection of the energy onto the zero-order modes are shown in Fig. 6. The apparent excitation of both modes, shaded columns, are substantial after the excitation of either mode. For the pumped mode the observable intensity change (shaded column), is not very different than that which would be predicted from using the zero-order modes, and calculating the intensity change due to the presence of excitation energy in the mode (unshaded column). In this case, the renormalization effect is a minor correction. However, for the mode which is not pumped, the renormalization effect dominates the observable intensity change shown by the shaded column; the effect of instantaneous energy transfer among the zero-order modes due to the dephasing process (unshaded column) is a minor contribution. Note also that the observable signal changes of the unpumped modes are in opposite directions for the two cases of pumping the (+) or the (−) mode. Excitation of the lower frequency mode leads to a positive apparent excitation of the higher frequency mode. A naive interpretation of an experimental measurement would indicate that substantial energy has transferred to the higher frequency mode, although in fact most of the apparent excitation is due to the changes in the normal modes. In contrast, excitation of the high-frequency mode leads to a negative apparent excitation (absorbance increase) of the lower frequency mode. This latter effect cannot be confused with energy transfer, and is a clear signature of the renormalization effect.

B. Normal modes and excitation of the H/Si(111) stepped surface

To calculate the Si–H stretching normal modes of the dihydride-stepped vicinal H/Si(111) surface, the $k=0$ mode of each oscillator row parallel to the step is modeled as a single oscillator, as in Sec. III B. The unit cell perpendicular to the step edge for the 9° cut surface is approximated as having seven oscillator rows, with the geometry shown in Fig. 7. The geometry is determined by the predictions of *ab initio* calculations,[16,23] which show a strong steric interaction between the first Si–H bond of the lower terrace and the dihydride on the step, causing a relaxation of the geometry of

the step Si–H bonds by a rotation toward the upper terrace. The vibrational motions shown in Fig. 7 represent the zero-order modes of the system in the absence of step-terrace dipole coupling. Each of the zero-order step modes is chosen to be the vibration of a single Si–H bond. This choice is somewhat different than the step normal modes given by the *ab initio* calculations,[23] but is in better agreement with the measured geometries of the step modes from recent Raman scattering[17,18] than are the *ab initio* results.[24] The four rows of terrace oscillators are chosen to be identical, consistent with the spectroscopic evidence that the terrace Si–H oscillators are all essentially identical to those of the flat surface.[20]

To apply the rows-as-oscillator model to this surface, the matrix **M** is a 7×7 matrix for the seven rows of Si–H bonds of Fig. 7. The interaction of row i with row j, f_{ij}, is obtained from Eq. (8); $U_{i \text{ row } j}(0)$ is obtained by summing the pairwise oscillator interactions over 50 lattice units of row j in each direction along the row, and by summing over 8 other rows j on equivalent terraces or steps; 4 each up and down the staircase (assuming all terraces in-phase; only the spectroscopically active $k=0$ modes are considered). Thus interaction with adjacent terraces and steps is included. The form of the interaction energy between each individual dipole m and dipole n that go into the row sums must take into account that the dipoles are not perpendicular to the surface, and is

$$U_{mn}=\frac{\mathbf{p}_m\cdot\mathbf{p}_n}{\mathbf{r}_{mn}^3}-3\,\frac{(\mathbf{p}_m\cdot\mathbf{r})(\mathbf{p}_n\cdot\mathbf{r})}{\mathbf{r}_{mn}^5}, \tag{16}$$

where $\mathbf{p}_i$ is the effective dipole vector, and $\mathbf{r}_{mn}$ is the inter-dipole vector. The source dipole m includes an enhancement of its vertical component by $(1+\kappa)=1.84$, and a decrease in its parallel component by $(1-\kappa)=0.16$, to approximate the effect of image dipoles. The focus is on the dipole interactions between the step and terrace modes. Within the steps themselves, the actual harmonic interactions that give rise to the step normal modes include both strong steric and kinetic coupling in addition to any dipole interactions. It would be very difficult to separate these effects, and we therefore do not attempt to model the dipole interactions among the step modes, or any changes in those interactions upon excitation. Instead, the final interaction matrix **M** has all direct couplings among the step oscillators set to zero, so that the final step modes, in the absence of step-terrace coupling, would remain single bond vibrations. This approach therefore gives final modes which are consistent with the observed geometries in Raman spectroscopy. The calculation will not, however, accurately reproduce intrastep intensity borrowing interactions. As we will show, however, it reproduces the qualitative features of the step-terrace interactions, and includes indirect coupling among step modes, mediated by the terrace oscillators.

The results for the normal modes of the ground state system are shown in Fig. 8. Consistent with the magnitudes of mixing observed in the two-row model of the last section, the modes are only slightly delocalized, with several percent of the energy of a step mode actually on terrace oscillators and vice versa. The intensity borrowing is however substantial. Figure 9 illustrates the unscreened effective dipole moments of the four modes before (dotted lines) and after (thin solid lines) the inclusion of dipole coupling. The thick solid lines represent the experimental measurements from internal

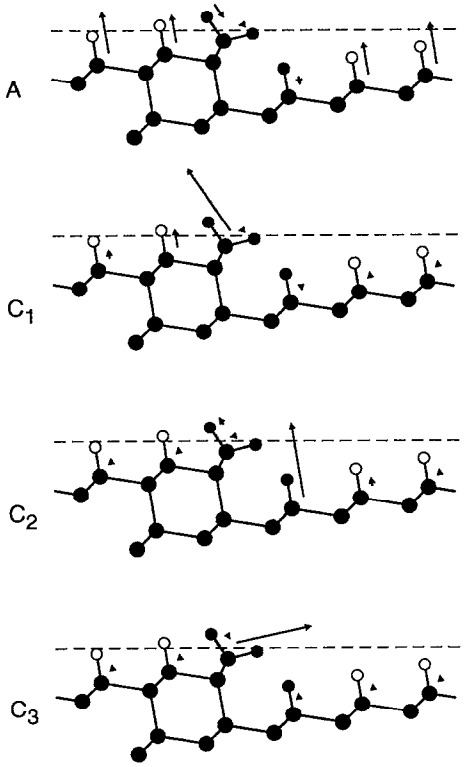

FIG. 8. Normal modes of the dihydride-stepped vicinal H/Si(111) 9° surface with terrace-step dipole coupling included.

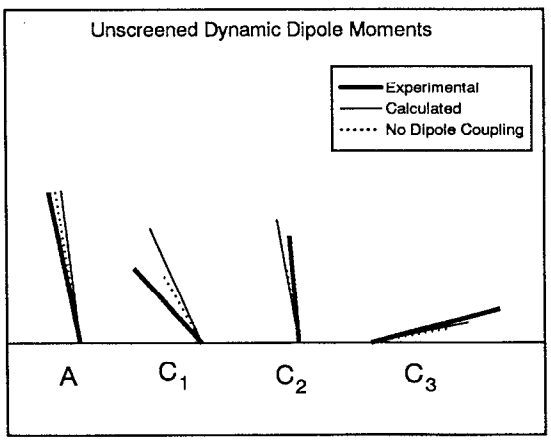

FIG. 9. Unscreened dynamic dipole moments of the Si–H stretching normal modes of the dihydride-stepped vicinal H/Si(111) 9° surface, with orientations shown with respect to the macroscopic surface plane. The mode dipole moments are calculated assuming that the dipole derivative of all Si–H bonds are identical. Dotted lines: dynamic dipole moments based upon zero-order normal modes, without terrace-step dipole coupling, as shown in Fig. 7. Thin solid lines: dynamic dipole moments based upon normal modes which include dipole coupling as shown in Fig. 8; thick solid lines: dynamic dipole moments measured by infrared spectroscopy (Ref. 25).

reflection infrared spectroscopy.[25] Only relative amplitudes are meaningful, so the A mode amplitude is scaled to be identical in the three cases. There is intensity transfer from the A mode into the C modes when dipole coupling is included. This qualitatively accounts for the observation that the intensity of the step modes is far greater than would be expected from their relative density on the surface. Overall, the dipole coupling leads to better agreement of the intensities with the experimental measurement. The quantitative agreement might well be improved further by the inclusion of intrastep coupling. We note that despite the substantial intensity borrowing, the orientation of the modes is not strongly affected by the dipole interactions.

Next, we consider the results of vibrational excitation on the normal modes of the stepped H/Si(111) surface, with an excitation of 0.10. The energy of excitation for each mode is projected incoherently onto the oscillator rows and the normal modes are recalculated. However, because of expected rapid energy diffusion on the terraces, the excitation energy of mode A is distributed equally among the oscillators of the terrace. Figure 10 presents the values of the apparent excitation of each mode (shaded columns) and the incoherent projection of the energy onto each mode due to dephasing (unshaded columns). As in the example of Sec. III, the renormalization is a small correction to the excitation of the pumped mode, but dominates the observed excitation for unpumped modes in comparison with energy transfer by dephasing alone. The renormalization again gives positive apparent excitation on modes at higher frequency than the one that is pumped, and negative apparent excitation on lower frequency modes. The largest effects come when A is pumped and the C modes are probed. This is because four oscillator rows are approximately equally involved in the A mode, so that an A mode excitation of almost 0.4 must be assumed in order that the net zero-order excitation is 0.1 after dephasing (four terrace modes are being excited by pumping the only one which is spectroscopically active.)

Particularly interesting in Fig. 10 are the values for the apparent excitation of A when the step modes C_1 and C_2 are pumped. These predict a negative apparent excitation of A, lasting as long as the step modes remain excited, consistent with the results shown in the experimental transients in Fig. 3. The predicted effects can be compared to the experimental results. We adopt the notation $X \rightarrow Y$ to refer to a pump mode X, probe mode Y experiment. For the data in Figs. 3 and 4, the ratio of the negative initial excitation in the experiment $C_2 \rightarrow A$ (-0.01) and the peak excitation observed in the experiment $C_2 \rightarrow C_2$ (0.12) is -0.08 and can be compared to the ratio of the corresponding values in Fig. 10, $-0.014/0.091 = -0.15$. No direct measurement for the $C_1 \rightarrow C_1$ experiment is available, because C_1 cannot be probed directly.[14] However, the estimated excitation in C_1 is similar or slightly higher than that of the C_2 mode, based upon its transition dipole. Therefore we expect the negative transient in $C_1 \rightarrow A$ compared to that in the experiment $C_2 \rightarrow A$ to scale roughly as the negative values in Fig. 10, or about 1.6 times larger. The actual ratio in the experimental results of Fig. 3 is a factor of 2 in the other direction. The order of magnitude of the negative transients is appropriate in both cases, and supports the argument that these negative transients arise from renormalization. The coupling strength in the calculation appears to be a factor of ~2 larger than that in the experiment, but this result is obtained without any adjustment of dynamic dipole moments or screening for the stepped surface vs the flat surface, and is well within the uncertainty of the model. The poor relative agreement of the negative transients on A after excitation of C_1 vs C_2 may indicate that the relative strengths of the calculated couplings for C_2 and C_1 with the A mode are not correct, and may be related to the absence of intrastep coupling in the model.

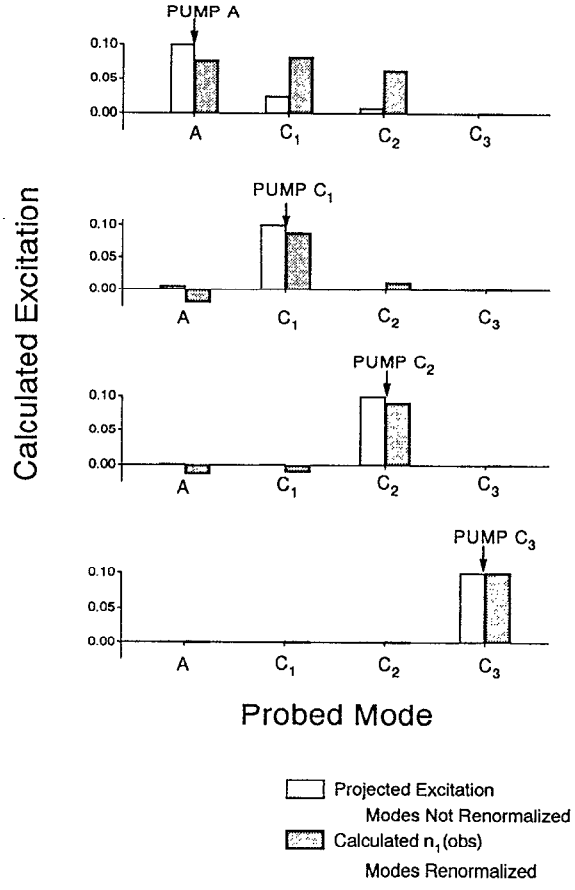

FIG. 10. Calculated excitation of the Si–H stretching normal modes of the dihydride-stepped vicinal H/Si(111) 9° surface (ground state modes are as shown in Fig. 8) after pumping each mode to a zero-order excitation of 0.10. Unshaded columns: excitation projected into each zero-order mode by the assumption that all oscillators lose phase coherence after the pumping process; shaded columns: the apparent instantaneous excitation n_1(obs), which would be observed in a transient experiment by an absorption probe following mode renormalization.

The interaction of the modes A and C_2 also occurs in reverse; when the lower frequency mode A is pumped, positive apparent excitation occurs in mode C_2. The calculated values from Fig. 10: $A \rightarrow C_2$ (0.063) and $A \rightarrow A$ (0.076) give a ratio of +0.82. Using the size of the negative transient in the reverse experiment as a guide, this calculated ratio is probably too large by a factor of 2. An estimate of ~0.4 can be compared to the experimental ratio from the measured excitation; $A \rightarrow C_2$ is 0.04 and $A \rightarrow A$ is 0.12, giving a ratio of

0.33. Therefore, the renormalization transient is predicted roughly to account for the entire observed signal change on mode C_2 following vibrational excitation of mode A! While there is considerable uncertainty in the calculated renormalization effect, this clearly indicates that a simple assignment of signal transients in this system to energy flow from one mode to another is not appropriate. Since both the renormalization and energy flow into C_2 will last as long as the long lifetime mode A is excited, the two effects cannot be easily distinguished in this case.

This result affects conclusions about energy flow on the surface. In particular, the original fit of a kinetic model for energy flow to the measured transients appeared to place too strong a coupling between A and C_2 in order to account for the large transient and its rapid rise.[14] Both of these effects can now be attributed at least in part to renormalization. A detailed refitting of this coupling would depend sensitively on the accuracy of the present calculation, which is poor, and such a calculation is therefore probably not justified. However, we emphasize that the existence of interadsorbate energy flow and estimates of the kinetic parameters can still be extracted from the data since the time scales of the transients due to renormalization are sometimes different [e.g., Figs. 3(a) and 3(b)], as discussed previously.[14] Quantitative conclusions will, however, be affected by the renormalization transients discussed here.

V. CONCLUSIONS

We have presented a simple technique to evaluate the role of vibrational excitation-induced renormalization of the vibrational modes in a dipole-coupled system. The method assumes that local dephasing of vibrational motions is rapid enough so that vibrational excitations can be considered as localized, incoherent excitations of single bonds on time scales longer than the dephasing time. The primary effect of excitation is to modify the effective charge of the excited oscillators, so that intralayer interactions are weakened. The resulting changes in the normal modes of the surface cause a reduction in intensity borrowing among the oscillators and therefore substantial spectral effects. The method is applied to the vibrational modes of the stepped vicinal H/Si(111) surface. The calculated intensity changes of the normal mode resonances on the dihydride-stepped surface following vibrational excitation are consistent with negative excitation transients observed in dynamic experiments. We emphasize that our previous discussion of a model for the energy diffusion by incoherent dipole–dipole coupling[13] which occurs after dephasing is not modified by the present discussion. The predicted intensity changes do however suggest that renormalization, which occurs on the time scale of vibrational dephasing, may interfere with the experimental study of such slower time scale effects as energy diffusion. Thus, although step-terrace energy flow has been confirmed for the stepped H/Si(111) surface,[14] some of the detailed kinetic parameters obtained in that work are questionable. More generally, the transient effects discussed here will be important in systems where the static spectrum shows intensity borrowing interactions.

[1] R. M. Hammaker, S. A. Francis, and R. P. Eischens, Spectrochim. Acta **21**, 1295 (1965).
[2] M. Moskovits and J. E. Hulse, Surf. Sci. **78**, 397 (1978).
[3] G. D. Mahan and A. A. Lucas, J. Chem. Phys. **68**, 1334 (1978).
[4] M. Scheffler, Surf. Sci. **81**, 562 (1979).
[5] B. N. J. Persson and R. Ryberg, Phys. Rev. B **24**, 6954 (1981).
[6] B. N. J. Persson and A. Liebsch, Surf. Sci. **110**, 356 (1981).
[7] See a general review in P. Hollins and J. Pritchard, Progr. Surf. Sci. **19**, 275 (1985).
[8] A. L. Harris, L. Rothberg, L. H. Dubois, N. J. Levinos, and L. Dhar, Phys. Rev. Lett. **64**, 2086 (1990); A. L. Harris, L. Rothberg, L. Dhar, N. J. Levinos, and L. H. Dubois, J. Chem. Phys. **94**, 2438 (1991).
[9] J. D. Beckerle, M. P. Casassa, R. R. Cavanagh, E. J. Heilweil, and J. C. Stephenson, Phys. Rev. Lett. **64**, 2090 (1990); J. D. Beckerle, R. R. Cavanagh, M. P. Casassa, E. J. Heilweil, and J. C. Stephenson, J. Chem. Phys. **95**, 5403 (19991).
[10] P. Guyot-Sionnest, P. Dumas, Y. J. Chabal, and G. S. Higashi, Phys. Rev. Lett. **64**, 2156 (1990); P. Guyot-Sionnest, P. Dumas, and Y. J. Chabal, J. Electron. Spectrosc. Relat. Phenom. **54/55**, 39 (1990).
[11] P. Guyot-Sionnest, Phys. Rev. Lett. **67**, 2323 (1991).
[12] M. Morin, N. J. Levinos, and A. L. Harris, J. Chem. Phys. **96**, 3950 (1992).
[13] M. Morin, P. Jakob, N. J. Levinos, Y. J. Chabal, and A. L. Harris, J. Chem. Phys. **96**, 6203 (1992).
[14] K. Kuhnke, M. Morin, P. Jakob, N. J. Levinos, Y. J. Chabal, and A. L. Harris, J. Chem. Phys. **99**, 6114 (1993).
[15] B. N. J. Persson, Phys. Rev. B **46**, 12,701 (1992).
[16] P. Jakob and Y. J. Chabal, J. Chem. Phys. **95**, 2897 (1991).
[17] M. A. Hines, T. D. Harris, A. L. Harris, and Y. J. Chabal, J. Electron. Spectrosc. Relat. Phenon. (in press).
[18] M. A. Hines, Y. J. Chabal, T. D. Harris, and A. L. Harris, Phys. Rev. Lett. **71**, 2280 (1993).
[19] Y. J. Chabal, Surf. Sci. Rep. **8**, 211 (1988).
[20] A similar rows-as-oscillators model was applied to calculate the frequency shifts for different terrace widths on the vicinal H/Si(111) surface; P. Jakob, Y. J. Chabal, K. Raghavachari, and S. B. Christman, Phys. Rev. B **47**, 6839 (1993).
[21] P. Jakob, Y. J. Chabal, and K. Raghavachari, Chem. Phys. Lett. **187**, 325 (1991).
[22] Ch. Stuhlmann, B. Bogdanyi, and H. Ibach, Phys. Rev. B **45**, 6786 (1992); see also Ref. 15.
[23] K. Raghavachari, P. Jakob, and Y. J. Chabal, Chem. Phys. Lett. **206**, 156 (1993).
[24] Calculations of the dipole coupling were also carried out using step modes as determined in the *ab initio* calculations. The magnitude of the predicted step-terrace coupling is 30%–50% less than that reported in this paper, and actually in better agreement with the transient measurements. The orientation of the mode dynamic dipole moments are, however, not in good agreement with the infrared absorption measurements in Fig. 9, or with the Raman measurements in Ref. 18.
[25] The dynamic dipole moments in Fig. 9 are based on remeasurements of spectra similar to those appearing in Ref. 16. The orientations are similar to those appearing in Table II of Ref. 16.